Molecular Pharmacology Fast Forward. Published on April 1, 2008 as doi:10.1124/mol.108.045674

MOL #45674

Identification of Regions Required for Apical Membrane Localization of Human Multidrug Resistance Protein (MRP) 2

Paul E. Bandler[1], Christopher J. Westlake[2], Caroline E. Grant, Susan P.C. Cole, and Roger G. Deeley

Division of Cancer Biology & Genetics, Queen's University Cancer Research Institute, Kingston, ON, Canada, K7L 3N6 (P.E.B., C.J.W., C.E.G., S.P.C.C., R.G.D.); Department of Pathology and Molecular Medicine (P.E.B., C.E.G., S.P.C.C., R.G.D.); Department of Biochemistry (C.J.W., R.G.D.)

Running title: Apical targeting of human MRP2

Address correspondence to: Roger G. Deeley, Division of Cancer Biology & Genetics, Queen's University Cancer Research Institute, Kingston, ON, Canada, K7L 3N6. E-mail: deeleyr@post.queensu.ca

Number of text pages: 36

Number of tables: 1

Number of Figs: 8

Number of references: 42

Number of words in *Abstract*: 250

Number of words in *Introduction*: 737

Number of words in *Discussion*: 1,599

ABBREVIATIONS: ABC, ATP-binding cassette; aa, amino acid; CL, cytoplasmic loop; ER, endoplasmic reticulum; $E_2$17βG, 17β-estradiol 17-(β-D-glucuronide); $E_1$3SO_4, estrone-3-sulfate; HRP, horseradish peroxidase; LTC_4, leukotriene C_4; MDCK, Madin-Darby canine kidney; MRP, multidrug resistance protein; MSD, membrane-spanning domain; PKC, Protein Kinase C; TB, transport buffer; TM, transmembrane.

ABSTRACT

Multidrug Resistance Proteins, MRP1 and MRP2, transport a wide range of endo- and xenobiotics. However, with the exception of certain parts of the brain, MRP1 traffics to basolateral membranes of polarized cells, while MRP2 is apical in location and thus is particularly important for systemic elimination of such compounds. Different regions of MRP1 and MRP2 appear to target them to their respective membrane locations. In addition to two 'core' membrane spanning domains (MSDs) characteristic of ABC transporters, MRP1 and MRP2 have a third NH_2-terminal MSD (MSD0), which, is not required for basolateral targeting of MRP1, or for transport of at least some substrates. Here, we demonstrate that all elements necessary for apical targeting of MRP2 reside in MSD0 and the adjacent cytoplasmic loop (CL) 3. Furthermore, we show that this region of MRP2 can target the 'core' of MRP1 to an exclusively apical location. Within MRP2 CL3, we identified a lysine rich element that is essential for apical targeting. When introduced into MRP1, this element alone is sufficient to result in partial apical localization. However, exclusive targeting to the apical membrane appears to require the integrity of the entire region encompassing MSD0 and CL3 of MRP2. Since CL3 of MRP1 is critical for binding and/or transport of a number compounds, we also examined the function of hybrids containing all, or portions of MRP2 MSD0 and CL3. Our results indicate that CL3 is important for interaction with both the GSH and glucuronide conjugates tested, but that different regions may be involved.

Multidrug resistance proteins MRP1(ABCC1) and MRP2 (ABCC2) are members of the 'C' branch of the ATP-binding cassette (ABC) transporter superfamily which includes 7 additional MRPs (ABCC4-6 and ABCC10-13), the cystic fibrosis transmembrane conductance regulator (CFTR/ABCC7) and the two sulfonylurea receptors (SUR1/ABCC8 and SUR2/ABCC9) (Deeley et al., 2006). MRP1 was discovered by virtue of its overexpression in the multidrug resistant human small cell lung cancer cell line, H69AR, and the presence of the protein in a number of types of cancers has since been correlated with poor prognosis (Deeley et al., 2006; Cole et al., 1992). MRP2 was initially identified by its similarity to MRP1 and subsequently shown to be defective in Dubin Johnson Syndrome, a rare congenital form of mild hyperbilirubinemia, as well as in naturally occurring strains of mutant rats which are defective in bile canalicular transport (Keppler et al., 1997; Paulusma et al., 1997).

MRP1 and MRP2 are 49% identical and have extensively overlapping substrate specificities, although their relative affinities for a given substrate often differ significantly. Both transport a wide range of glutathione (GSH), glucuronate and sulphate conjugated organic anions, as well as other unconjugated organic anions, such as methotrexate (Leslie et al., 2005; Qian et al., 2001b; Deeley et al., 2006). They are also capable of GSH-stimulated transport of various hydrophobic chemotherapeutic drugs, including anthracyclines and *Vinca* alkaloids (Deeley et al., 2006). However, MRP1 and MRP2 differ markedly with respect to their tissue distribution and subcellular location. MRP1 is expressed in a wide range of tissues and in general traffics to basolateral membranes, while MRP2 is found exclusively in the apical membranes of secretory epithelia, primarily in the liver, gallbladder, kidney, small intestine, colon, placenta and lung (Keppler et al., 1997; Van Aubel et al., 2000). Thus although both proteins contribute to cellular efflux of a wide range of phase II metabolites, as well as unconjugated drugs and toxins, MRP2 is particularly important for the elimination of these compounds.

In addition to two membrane spanning domains (MSDs) and two cytoplasmic nucleotide binding domains (NBDs) characteristic of ABC transporters, some ABCC proteins, including MRP1and MRP2, have an additional NH2-terminal MSD (MSD0) (Hipfner et al., 1997; Tusnady et al.,1997). MSD0 is required for appropriate trafficking and targeting of MRP2, as well as other ABCC proteins, such as SUR1 (Babenko and Bryan, 2003) and the yeast MRP1 ortholog, YCF1 (Mason and Michaelis, 2002). In contrast, human MRP1 lacking MSD0 traffics to basolateral membranes and is capable of transporting LTC_4 and certain other substrates (Bakos et al., 1998; Westlake et al., 2003). This may be attributable to redundant trafficking determinants present in both MSD0 and the COOH-terminal region of MRP1 (Westlake et al., 2005). Unlike MSD0 from MRP2, MRP1 MSD0 traffics efficiently to the plasma membrane in the absence of the 'core' of the protein, (Fernandez et al., 2002; Bakos et al., 1998; Westlake et al., 2005).

The COOH-terminal regions of both MRP1 and MRP2 have been implicated in targeting these proteins to their respective locations in the plasma membrane (Westlake et al., 2004). This region of MRP2 contains a putative PDZ binding motif which could target the protein to the apical membrane *via* interaction with scaffolding proteins such as radixin. In support of this suggestion, localization of MRP2 to the hepatocanalicular membrane is impaired in radixin knock out mice (Kikuchi et al., 2002). However, the COOH-terminal 70-75 aa of MRP1 and MRP2 can be exchanged without affecting localization of either protein (Westlake et al., 2004). Similarly, reciprocal exchange of MSD0 between the two proteins is not sufficient to alter polarized membrane targeting of the two proteins (Konno et al., 2003; Westlake et al., 2005). Thus other regions of MRP1 and MRP2 must contribute to, or be essential for, determining their different subcellular localization.

Using hybrid proteins, we demonstrate that aa 1-319 of MRP2, which includes MSD0 and the cytoplasmic loop (CL3) connecting it to the remainder of the protein, contain all of the targeting elements necessary to redirect the core region of MRP1 from a basolateral location exclusively to the apical membrane. Within CL3 of MRP2, we identify a lysine rich element between aa 294-303 that is unique among the MRPs and which is essential for apical targeting of MRP2. This element alone is sufficient to partially redirect MRP1 to an apical location. However, the integrity of the region spanning MSD0 and CL3 appears to be essential for targeting the protein exclusively to the apical membrane.

Materials and Methods

ATP, AMP, Dulbecco's SP modified Eagle's medium, F-12 nutrient supplement, Grace's Medium, Kanamycin, LTC_4, E_13SO_4, S-methyl-GSH, 4-azidophenacylbromide, glutathione reductase and NADPH tetrasodium salt were purchased from Sigma-Aldrich (St. Louis, MO). [^{3}H]LTC_4 (167.5 Ci/mmol), [^{3}H] E_13SO_4 (57.3Ci/mmol), [^{3}H]$E_2$17βG (53 Ci/mmol) and [^{35}S]GSH (1498 Ci/mmol) were purchased from Perkin-Elmer Life Sciences (Waltham, MA). MRP1-specific monoclonal antibodies (mAb) used for immunoblotting or immunocytochemistry were: MRPr1 (rat) and MRPm6 (mouse) (Alexis Biochemicals, San Diego, CA) and QCRL-1 (mouse) (previously described in (Hipfner et al., 1996 and 1998), and a poly-clonal, Rabbit anti-calnexin antibody (Sigma-Aldrich). The MRP2-specific mAb used was $M2_{I-4}$ (mouse) (Alexis Biochemicals, San Diego, CA). Conjugated antibodies used for immunofluorescent detection were: Alexa 488 goat anti-mouse/rat and Alexa 594 goat anti-rabbit (Molecular Probes Inc., Carlsbad, CA). Hoechst 33342 nuclear stain was also obtained from Molecular Probes Inc. Goat-anti-mouse/rat/rabbit IgG (H+L) conjugated with horseradish peroxidase (Pierce Biotechnologies Inc., Rockford, IL) was used as a secondary antibody. Immobilon-P membranes and chemiluminescence HRP substrate (Millipore, Billerica, MA) were used for detection in immunoblotting. All restriction endonucleases were purchased from New England Biolabs Inc. (Ipswich, MA).

Generation of MRP1/MRP2 Chimeric or Truncated Constructs. pcDNA3.1(-) vectors for expression of full-length MRP1 and MRP2 have been described previously (Ito et al., 2001, Westlake et al., 2004). The strategy for constructing expression vectors for MRP1/MRP2 hybrids is summarized in Table 1. Briefly, fragments corresponding to specific portions of MRP1 or MRP2 were generated by PCR amplification using primers with 'tails' complementary

to hybrid junctions listed in Table 1. Appropriate amplified DNA products were then mixed, denatured, re-annealed and used as a template to generate the required hybrid fragment using ProofStart™ enzyme (Qiagen, Mississauga, ON). Each recombinant DNA fragment was then amplified by PCR using primers indicated in boldface in Table 1 and inserted into the respective vector backbone *via* restriction digests as indicated (Table 1).

$MRP2_{1-319}$ was generated by PCR amplification of the corresponding cDNA from pcDNA3.1(-)-MRP2 with the forward primer 5'-GCTCTCTGGCTAACTAGAGAACC-3' in pcDNA3.1 and the reverse primer 5'-CGGCCGCCTAGTAGAAAGTTTTGAACAG AGCC-3' which resulted in addition of a stop codon and a NotI site (underlined) following the codon for Tyr319. The PCR product was digested with NheI and NotI and cloned into pcDNA3.1(-). $MRP1_{1-203}$/$MRP2_{189-319}$/$MRP1_{323-1531}$ was generated by ligation of the small fragment from *SacI*-digested pcDNA3.1(-)$MRP1_{1-203}$/$MRP2_{189-1546}$ (Westlake et al., 2005) to the *SacI*-digested hybrid construct pcDNA3.1-$MRP2_{1-319}$/ $MRP1_{323-1531}$ (described in Table 1). The cDNAs of hybrid molecules intended for viral infection of insect cells and vesicular transport assays were cloned into pFastBac vector after digestion with *XbaI/KpnI*. The fidelity of all constructs was confirmed by DNA sequencing.

Generation of Mutants in the $MRP2_{1-319}$/$MRP1_{323-1531}$ Hybrid Construct. The QuikChange® XL Site-Directed Mutagenesis Kit (Stratagene, La Jolla, CA) was used according the manufacture's protocol to generate all mutant proteins. The codon for Lys296 in pcDNA3.1(-)$MRP2_{1-319}$/$MRP1_{323-1531}$ was mutated to arginine with F:5'-GAAACGCAAGA AGTCTGGG-3'/ R:5'-CCCAGACTTCTTGCGTTTC-3', to glutamine with F:5'-GAAA CAGAAGAAGTCTGGG-3'/ R:5'-CCCAGACTTCTTCTGTTTC or to glutamate with F: 5'-GAAAGAGAAGAAGTCTGGG-3'/ R:5'-CCCAGACTTCTTCTCTTTC. Residues 294-303 in

the $MRP1_{1-319}$ hybrid were also mutated to the corresponding MRP1 sequence in the same manner, with the following primers: F:5'-GATGTTGAAAAGGAGTGGAACCCCTCTCTG TTTAAGGTGGATGTTCCA-3'/ R:5'-TGGAACATCCACCTTAAACAGAGAGGGGTT CCACTCCTTTTCAACATC-3'. The fidelity of all constructs was confirmed by DNA sequencing.

Expression and Localization of MRP1/2 Hybrid and/or Mutated Proteins in Mammalian Cells. MRP1/MRP2 hybrids were expressed in stably transfected MDCK-1 cells and transiently transfected LLC-PK1 cells. Additional mutant-hybrid constructs were expressed in transiently transfected MDCK-1 cells. Cells were cultured in DMEM with 10% fetal bovine serum which was supplemented with F-12 nutrient mix when used for LLC-PK1 cells. Transfections were performed using Lipofectamine 2000® (Invitrogen, Carlsbad, CA) reagent according the manufacturer's instructions. Stably transfected MDCK-1 cells were obtained by selection in Geneticin (Gibco, Auckland, NZ) (800 μg/mL) for two weeks, followed by limited dilution to isolate clonal populations which were then maintained in Geneticin supplemented medium. To assess MRP1 protein expression, cells were grown to confluence in 15 cm dishes, then harvested in ice-cold PBS containing Complete Protease Inhibitor® (Roche Diagnostics, Mississauga, ON) by scraping the dish with a rubber policeman. Cells were washed and lysed by incubation on ice in buffer containing 10 mM tris (pH 7.5), 10 mM KCl, 1.5 mM $MgCl_2$ and protease inhibitors for 10 min. Total cellular membranes were then isolated by centrifugation. Membrane proteins were resolved by 7.5% SDS-PAGE and blots were probed with mAb MRPm6 or mAb $M2_{I-4}$. A mouse or rat IgG secondary antibody conjugated to horseradish peroxidase (HRP) was applied and antibody-protein interactions were detected using a chemiluminescent substrate for HRP.

For protein localization studies, cells were seeded onto glass coverslips and allowed to become confluent over 7-9 days at 37°C in 5% CO_2. Cells were then fixed with cold 95% ethanol and proteins were detected with mAb MRPr1 or mAb M2I-4 and goat anti-rat Alexa 488 or goat anti-mouse Alexa 488 respectively. Cells were also stained with a rabbit polyclonal antibody to the endoplasmic reticulum marker, calnexin, which was detected with goat anti-rabbit Alexa 594 as described (Westlake et al., *2*003). Cell nuclei were stained with Hoechst 33342. Fluorescent antibodies were detected with a Leica TCS SP2 dual photon confocal microscope.

Viral Infection, Membrane Vesicle Preparation and Immunoblotting. Generation of baculovirus from recombinant bacmids and methods for infection of Sf21 cells have been described previously (Gao et al., 1996). Membrane vesicles were prepared from infected insect cells by nitrogen cavitation at 200 psi for 5 min and followed by sucrose density centrifugation (Gao et al., 1996). Membrane proteins were resolved by 7.5% SDS-PAGE and MRP levels were determined by immunoblotting and densitometry. Slot blots were performed with a Bio-Rad Bio-Dot® SF microfiltration apparatus (Bio-Rad, Richmond, CA) according to the manufacturer's instructions.

ATP-dependent Uptake of LTC_4, E_13SO_4 and $E_217\beta G$ Transport by MRP1 and Hybrids across Sf21 Membranes. MRP mediated uptake of various substrates by membrane vesicles from Sf21 cells was determined using a rapid filtration assay (Gao et al., 1996) at 23°C as described. Briefly, Sf21 membrane vesicles (4 μg total protein) were incubated at 23°C in transport buffer (50 mM Tris, 250 mM sucrose, pH 7.4) containing [^{3}H]LTC_4 (50 nM, 10 nCi/reaction), AMP or ATP (4 mM) and $MgCl_2$ (10 mM). ATP-dependent transport was determined by subtracting the uptake in the presence of AMP from the uptake in the presence of ATP. ATP-dependent uptake of [^{3}H]E_13SO_4 (300 nM, 50 nCi/reaction) or [^{3}H]$E_217\beta G$ (400 nM,

25 nCi/reaction and 6 μg of protein) was measured at 37°C in a similar manner. For the transport of E_13SO_4, reactions were supplemented with 2 mM S-methyl-GSH (Qian et al., 2001a).

Synthesis of Azidophenacyl-[^{35}S]GSH. Synthesis of azidophenacyl-[^{35}S]GSH was carried out as described (Qian et al., 2001a). Briefly, 100 μCi of stock [^{35}S]GSH (1498 Ci/mmol) was extracted with ethyl acetate to remove dithiothreitol and diluted to 500 Ci/mmol with cold GSH (Sigma-Aldrich, St. Louis, MO). This was added to a reaction mixture containing N_2 saturated, degassed PBS, 4-azidophenacylbromine (4 mM), 125 mU of GSH-reductase and 1 mM NADPH for 1 hr at room temperature. Products were separated by silica-G thin layer chromatography (TLC) using i-propanol/water/acetic acid (12:5:1, v/v/v). Spots exhibiting the appropriate mobility on the TLC plate (R_f ~ 0.6) were confirmed to contain azidophenacyl-[^{35}S]GSH by autoradiography, then scrapped off the plate and extracted 6 times with 400 μL of water. Extracts were concentrated under a stream of nitrogen.

Photolabeling of MRP1 and Hybrids with Azidophenacyl-[^{35}S]GSH. Membranes (~75 μg total protein) from Sf21 cells expressing MRP1 and various hybrid proteins were incubated with azidophenacyl-[^{35}S]GSH (0.5 μCi) at room temperature for 10 min in transport buffer (50mM Tris, 250mM sucrose, pH 7.4) and then UV-irradiated (312 nM) for 5 min on ice. Membrane proteins were analyzed by SDS-PAGE (10% acrylamide) after solubilization in Laemmli's buffer. Gels were treated with Amplify™ (Amersham Biosciences, Piscataway, NJ), dried and autoradiography was performed at -70°C. Exposure times ranged from 1 to 3 days.

Results

Expression and Subcellular Localization of MRP1/MRP2 Hybrid Proteins in Polarized Epithelial Cells. Previously, we have shown that substitution of MSD0 of MRP1 with MSD0 of MRP2 has no effect on trafficking of the protein to its normal location in the basolateral membranes of polarized MDCK-1 cells (Westlake et al., 2005). However, these studies also demonstrated the importance of parts of the cytoplasmic region (CL3) that links MSD0 and MSD1, both with respect to processing through the endoplasmic reticulum (ER) and subsequent trafficking of MRP1 to the basolateral membrane. Fig. 1 shows an alignment of CL3 from human MRPs 1, 2 and 6 and the yeast MRP1 ortholog, YCF1, with the cytoplasmic amino termini of human MRP4 and CFTR. It also illustrates the relatively conserved N-proximal region of CL3 referred to above and the divergence of the C-proximal portions of the aligned regions (Westlake et al., 2005).

To investigate the possible importance of MRP2 CL3 for apical targeting, we constructed various MRP1/MRP2 hybrids or truncated proteins and expressed them in polarized epithelial cells. The multiple sequence alignments of CL3 (Fig. 1) were used to identify points for connecting various fragments in the hybrid proteins, taking care to maintain predicted conserved secondary structures shown and to minimize loss or duplication of homologous sequences. The hybrids generated are illustrated in Fig. 2. Two polarized kidney epithelial cell lines that reportedly differ in their sorting mechanisms were used to compare trafficking of the hybrids with that of wild-type MRP1 and MRP2 (Roush et al., 1998). Fig. 3 shows confocal micrographs of the wild-type proteins stably expressed in MDCK-1 (canine) and transiently expressed in LLC-PK1 (porcine) cells. As expected from previous studies, MRP1 and MRP2 localized exclusively to the basolateral or apical plasma membranes of both cell types, respectively. We

next examined the polarized sorting of several MRP1/MRP2 hybrid molecules (constructs A, B, and C shown in Fig. 2) in stably transfected MDCK-1 cell lines (Fig. 4). Previously, we have shown that exchange of the first 280 aa of MRP1 for those of MRP2 resulted in a protein that was inactive when expressed in Sf21 insect cells and which failed to exit the ER in mammalian cells (Gao et al., 1998). Consequently, we initially extended the substituted region so that aa 1-289 of MRP2 replaced aa 1-290 of MRP1 ($MRP2_{1-289}$/ $MRP1_{291-1531}$) (Fig. 2B). However, this hybrid protein also remained trapped in the ER, as evidenced by colocalization with the ER marker calnexin (Fig. 4A, left panel). In contrast, substitution of the first 319 residues of MRP2, which includes essentially all of MSD0 and CL3, for aa 1-322 of MRP1 ($MRP2_{1-319}$/ $MRP1_{323-1531}$) (Fig. 2A) resulted in apical sorting of the hybrid (Fig. 4B, left panel). No evidence of the presence of the hybrid in basolateral membranes could be detected by confocal microscopy.

The results of studies with hybrids $MRP2_{1-289}$/ $MRP1_{291-1531}$ and $MRP2_{1-319}$/ $MRP1_{323-1531}$ suggested that a crucial element for apical sorting in MRP2 was located between aa 290-319. To test this possibility, a hybrid was constructed in which 34 aa from CL3 (residues 286-319) of MRP2 was substituted for the region in MRP1 corresponding to aa 291-322 ($MRP1_{1-290}$/$MRP2_{286-319}$/$MRP1_{323-1531}$, Fig. 2C). This construct trafficked to the plasma membrane and was readily detectable in the apical component. However, unlike the construct containing MSD0 and all of CL3 from MRP2, this hybrid was also present in basolateral membranes (Fig. 4C, left panel). Thus its distribution was intermediate between those of wild-type MRP1 and MRP2.

To determine whether similar behaviour was observed in LLC-PK1 cells, we generated transient transfectants using the same set of hybrids (Fig. 4A,B and C, right panels). All of the constructs displayed the same sorting profiles observed in the MDCK-1 cells, including combined apical and basolateral localization of the $MRP2_{286-319}$ hybrid. These findings indicate

that the region encompassing residues 286-319 in MRP2 contains elements that are necessary for apical sorting of the protein. These elements are also sufficient to target a substantial fraction of MRP1 to the apical membrane, albeit with reduced efficiency when compared with a hybrid containing all of MSD0 and CL3 from MRP2.

Functional Interaction of COOH-proximal End of CL3 with other Regions in CL3 or MSD0. To further investigate the role of the COOH-proximal end of MRP2 CL3 in apical sorting, stable MDCK-1 cell lines were created expressing one of four additional MRP1/MRP2 hybrids (Fig. 2D-G). Polarized sorting was then examined as described above. First, we determined whether the region between aa 286-319 was essential for apical targeting of MRP2 by exchanging this region for aa 291-322 of MRP1 ($MRP2_{1-289}/MRP1_{291-322}/MRP2_{320-1546}$) (Fig. 2D). Confocal microscopy revealed that this substitution severely impaired apical trafficking (Fig. 5A, left panel). However, this hybrid did not co-localize with calnexin indicating that it was able to exit the ER. Instead, the protein was apparently retained in an intracellular vesicular compartment. Thus the results support the importance of the region between aa 286-319 of MRP2 for targeting to the apical plasma membrane.

In view of the results obtained with hybrid $MRP2_{1-319}/ MRP1_{323-1531}$ and the previous observation that MSD0 of MRP2 is required for trafficking to, and retention in, the plasma membrane (Fernandez et al., 2002), we generated a hybrid ($MRP2_{1-187}/MRP1_{204-290}/MRP2_{286-319}/MRP1_{323-1531}$) that contained all of MRP2 MSD0 ($MRP2_{1-187}$) together with $MRP2_{286-319}$. However, this hybrid had a plasma membrane distribution that was indistinguishable from the hybrid containing only $MRP2_{286-319}$ (Fig. 5B, left panel). Thus, despite the requirement of MSD0 for the trafficking of MRP2 to the plasma membrane, its inclusion did not detectably increase the apical location of the hybrid MRP1 protein when compared with $MRP1_{1-290}/MRP2_{286-}$

$_{319}$/MRP1$_{323-1531}$ (Fig. 4C, left panel). To determine whether NH_2-proximal regions of CL3 of MRP2 were also required for apical targeting, we constructed a hybrid in which all of CL3 of MRP1 was replaced with CL3 from MRP2 (MRP1$_{1-203}$/MRP2$_{189-319}$/MRP1$_{323-1531}$) (Fig. 5C, left panel). Like the construct containing MSD0 of MRP2 (Fig. 5B, left panel), the plasma membrane distribution of this hybrid was essentially unchanged from that of MRP1$_{1-290}$/MRP2$_{286-319}$/MRP1$_{323-1531}$ (Fig. 4C, left panel).

We and others have previously shown that MSD0 of MRP1 alone or connected to various segments of CL3 can traffic independently to basolateral membranes. In contrast, Fernandez et al., (2002) reported that MRP2$_{1-305}$ was retained in an intracellular compartment in MDCK-II cells and failed to reach the plasma membrane. Having determined that MRP2$_{1-319}$ contained all the information necessary to direct MRP1 exclusively to the apical membrane, we determined whether MRP2$_{1-319}$ was independently capable of apical trafficking. However, this construct was found to colocalize predominantly with calnexin indicating that it was retained in the ER (Fig. 5D, left panel). As with the initial set of hybrids, trafficking of these four constructs was also examined by transient expression in LLC-PK1 cells (Fig. 5A-D, right panels). The distribution in LLC-PK1 cells did not differ from that observed in MDCK-1 cells, with the exception of MRP2$_{1-319}$ which had a punctate, intracellular, vesicular-like distribution, as opposed to being retained in the ER.

Overall, these results support the suggestion that a critical region for apical trafficking lies between aa 286 and 319 in MRP2, but they also indicate that additional interactions involving both MSD0 and the NH_2-proximal half of CL3 may be required for full localization to, or retention in, the apical membrane. The fact that MRP2$_{1-319}$ does not traffic independently also raises the possibility of a requirement for additional processing and trafficking signals present in

the core regions of both MRP1 and MRP2, or that the presence of the core regions of the proteins is required for the correct folding of $MRP2_{1-319}$.

Impact of Mutations in CL3 on the Apical Localization of $MRP2_{1-319}$/$MRP1_{323-1531}$ in Transiently Transfected MDCK-1 Cells. Sequence alignments of CL3 from several MRPs and related proteins (Fig. 1) reveal a unique polybasic motif from residues 294-303 in MRP2. This motif falls within the small region of MRP2 ($MRP2_{286-319}$) shown above to be capable of causing partial redistribution of MRP1 to the apical membrane when introduced into that protein. Polybasic motifs, such as the one present in MRP2 CL3, are potential sites for membrane interaction (Heo et al., 2006). Consequently, we performed a series of mutations within this polybasic motif in the $MRP2_{1-319}$ hybrid which we showed above contains all the necessary components to redirect MRP1 exclusively to the apical membrane in polarized cells. Lysine at position 296 of the hybrid protein was arbitrarily selected since it is located in the middle of a stretch of five lysine residues in the polybasic motif (KK**K**KKSGTKK, Fig. 1) and was mutated to arginine, glutamine or glutamate, and transiently expressed in MDCK-1 cells. In addition, we exchanged the whole basic motif (aa 294-303) for the most closely corresponding region in MRP1 (aa 299-308).

Confocal micrographs shown in Fig. 6 demonstrate that point mutations at K296 do not affect the apical trafficking of this hybrid regardless of the level of conservation of the mutation. In contrast, when the whole motif was mutated in the hybrid, a large proportion of the protein was localized in an (subapical) intracellular component. However, it was not retained in the ER, since it did not colocalize with calnexin (Fig. 6). Thus the hybrid lacking the basic motif is able to exit the ER but either fails to be targeted to, or retained in, the apical membrane.

LTC_4 and $E_2$17βG Transport by MRP1/MRP2 Hybrid Proteins. CL3 of MRP1 is important, not only for trafficking of the protein but also the binding and/or transport of substrates such as LTC_4 and azidophenacyl-GSH (Gao et al., 1998; Qian et al., 2002). The region of CL3 required for activity extends from amino acid 208 to 260, while that necessary for efficient trafficking is somewhat longer and extends an additional 9 aa to 269 (Westlake et al., 2003). Given the functional importance of CL3 of MRP1 and the relatively low sequence identity of this region between MRP1 and MRP2 (30%), we investigated whether those hybrids in which various regions of CL3 had been exchanged retained transport activity when expressed in insect Sf21 cells (Fig. 7). Previous studies of mutant or hybrid forms of MRP1 have revealed that efficient processing and the ability to traffic to the plasma membrane does not necessarily indicate that the proteins are functional. Conversely, an inability to traffic appropriately in mammalian cells does not preclude the possibility that the protein may be capable of folding into an active conformation when expressed in insect cells.

Expression levels of the hybrid proteins were assessed by SDS-PAGE followed by immunoblotting and the relative levels of the proteins were determined by densitometry of slot-blots of membrane vesicles prepared from infected cells (Fig. 7A, B). Expression levels of hybrid proteins ranged from approximately 10% to 40% higher than that of wild-type MRP1. The transport activity of the hybrids relative to wild-type MRP1 was assessed by measuring ATP-dependent uptake of LTC_4 or $E_2$17βG by inside-out membrane vesicles prepared from infected cells. The extent of uptake was then normalized to compensate for minor differences in the level of protein expression between the hybrids and wild-type MRP1.

Data in Fig. 7 (panels D and E) are combined from two separate experiments and show time courses of LTC_4 uptake by MRP1 and hybrid proteins at 23^{o}C. Hybrids with MRP1 regions

substituted for $MRP2_{286-319}$ or $MRP2_{1-319}$ demonstrated normalized transport levels that were approximately 60% and 30% of wild-type MRP1 respectively (Fig. 7D). While both $MRP2_{286-319}$ and $MRP2_{1-319}$ hybrids retained some ability to transport LTC_4, transport of $E_217\beta G$ could be detected only with the $MRP2_{286-319}$ hybrid, but was approximately 25% as active as wild-type MRP1 (Fig. 7C). Taken together, these findings suggest that different regions of CL3 may be important for the transport of these two substrates.

Although both MRP1 and MRP2 transport LTC_4, previous kinetic analyses indicate that the apparent affinity of MRP2 for this substrate is approximately 10-fold lower than that of MRP1 (Cui et al., 1999). Consequently, we determined how the introduction of regions from MRP2 affected the kinetic parameters of LTC_4 transport by the $MRP2_{286-319}$ and $MRP2_{1-319}$ hybrids (Fig. 7E). The K_m and V_{max} of wild-type MRP1 for LTC_4 were determined to be 83 nM and 89 pmol/min/mg vesicle protein, respectively, and were similar to our previously published values (Gao et al., 1996). Introduction of $MRP2_{286-319}$ increased the K_m to approximately 220 nM without a detectable change in V_{max}, whereas K_m of the hybrid containing the $MRP2_{1-319}$ substitution increased to approximately 710 nM. The normalized V_{max} of this construct was modestly increased to120 pmol/min. Thus introduction of the limited $MRP2_{286-319}$ region decreased the apparent affinity for LTC_4 approximately 2.5 fold, while exchange of the entire MSD0/CL3 region decreased the apparent affinity 8-9 fold.

GSH Binding and E_13SO_4 Transport by MRP1/MRP2 Hybrid Proteins. Since transport of the GSH-conjugated LTC_4 was readily detectable with both hybrids, we evaluated the ability of the hybrid proteins to transport the GSH dependent substrate E_13SO_4. Previously, we have shown that transport of E_13SO_4 by MRP1 is stimulated 5-10 fold in the presence of GSH or S-methyl GSH (Qian et al., 2001a). In contrast, this conjugate is not a substrate for

MRP2, either alone or in the presence of GSH. ATP-dependent uptake of E_13SO_4 (300 nM) into Sf21 membrane vesicles was measured after incubation at 37^{o}C for 3 min in the presence of 2 mM S-methyl GSH (Qian et al., 2001a). Fig. 8A shows that uptake by the hybrid containing $MRP2_{286-319}$ was markedly reduced to approximately 10% that of wild-type MRP1 (8 pmol/mg/3min), while transport by the $MRP2_{1-319}$ hybrid was not detectable.

We have shown previously that CL3 of MRP1 is required for binding of the photoactivatable derivative of GSH, azidophenacyl-GSH, although no direct labeling of this region of the protein could be detected (Qian et al., 2002). Presently, nothing is known of the elements in MRP2 that are required for interaction with GSH which has been reported to be a low affinity substrate for the protein (K_m 19 mM) (Paulusma et al., 1999). To determine whether the reduction of E_13SO_4 transport by the hybrid proteins might be attributable to loss of GSH binding, we carried out a photolabeling study with azidophenacyl-[^{35}S]GSH (Ciaccio et al., 1996), which has previously been established as a functional, non-reducing substitute for GSH (Qian et al., 2002). As shown in Fig. 8B, and as we have previously reported, wild-type MRP1 expressed in Sf21 membrane vesicles was clearly labeled with azidophenacyl-[^{35}S]GSH (Qian et al., 2002). Photolabeling of the MRP1 hybrid containing $MRP2_{1-319}$ was barely detectable while photolabeling of the $MRP2_{286-319}$ substituted protein was only modestly affected.

Discussion

MSD0 and the COOH-terminal region of MRP1 contain at least partially redundant processing/trafficking signal(s) (Westlake et al., 2004 and 2005). This redundancy explains, at least in part, the ability of MRP1 to traffic to the basolateral plasma membrane in the absence of MSD0. The regions involved in targeting MRP2 to apical membranes have been less well defined but clearly differ from those identified in MRP1. MRP2 accumulates in intracellular vesicles when expressed in the absence of MSD0 suggesting that this region may contain trafficking/targeting signals (Fernandez et al., 2002). However, Konno et al., (2003) found that MRP1/MRP2 hybrids containing the NH_2-terminal 240 aa from MRP1, which includes MSD0 and 37 aa of CL3 trafficked normally, while a hybrid in which the NH_2-terminal 480 aa were exchanged failed to reach the apical membrane. These results suggest that a signal(s) essential but not necessarily sufficient for the apical location of MRP2 may be located between aa 240-480 which encompasses the C-proximal 79 aa of CL3 and TMs 6-9 of MSD1. The importance of the putative PDZ binding motif in the COOH-terminal region of MRP2 remains controversial, since this element can be deleted without altering the apical localization of the protein (Nies et al., 2002). Similarly, introduction of this region into MRP1 fails to change the protein's basolateral location (Westlake et al., 2005).

Rather than inferring the presence of targeting signals from a loss of targeting specificity, we sought to identify regions and/or elements in MRP2 that were sufficient to redirect the core region of MRP1 from the basolateral to the apical membranes of two polarized kidney cell lines. We began by investigating the importance of MSD0 and CL3. The primary sequence conservation of MSD0 among the ABCC proteins is low and MSD0 of MRP2, unlike MSD0 from MRP1, is unable to traffic independently to the plasma membrane although it is processed

through the ER (Fernandez et al., 2002; Westlake et al., 2005). Sequence conservation within CL is also relatively low. However, within CL3, several secondary structure algorithms predict the presence of two α-helical motifs that are conserved even in distantly related MRP orthologs and homologs (Fig. 1) (Westlake et al., 2003; Bakos et al., 2000). In MRP1, residues 208-269 of CL3, which include both conserved helices, are critical for ER processing (Westlake et al., 2003; Bakos et al., 2000).

We have shown previously that exchange of the first 280 aa of MRP1 for the comparable region of MRP2, results in a protein that fails to exit the ER in mammalian cells and is inactive when expressed in insect Sf21 cells (Gao et al., 1998). Extending the exchanged region to residue 289 did not prevent the hybrid from being trapped in the ER (Fig. 3) and this hybrid was also inactive in Sf21 cells (data not shown). In contrast, a MRP1 hybrid containing $MRP2_{1-319}$ was able to exit the ER and localized exclusively to the apical membrane in both MDCK-1 cells and LLC-PK1 cells (Fig. 4). Thus, $MRP2_{1-319}$, which includes MSD0 and the whole of CL3, contains all components necessary to efficiently redirect the core of MRP1 to the apical membrane. Furthermore, inclusion of the COOH-proximal region of MRP2 CL3 (aa 289-319) appears to be required for appropriate folding and processing of the hybrid protein through the ER.

The above results suggested that aa 290-319 of MRP2 CL3 were involved in targeting the protein to the apical membrane. Consistent with this possibility, a substantial fraction of a MRP1 hybrid containing only these twenty aa localized to apical membranes (Fig. 4C). Although not sufficient to redirect MRP1 exclusively to the apical membrane, the reciprocal substitution of this region of MRP2 with the corresponding region of MRP1 (Fig. 5A), indicated that it was essential for apical targeting, either directly from the Golgi or *via* transcytosis. The lack of apical

localization of the mutated MRP2 was not simply attributable to mis-folding since the protein was able to exit the ER, but accumulated in an intracellular vesicular compartment rather than the apical membrane. Furthermore, no trace of the MRP2 mutant was detectable on the basolateral membrane, suggesting that a direct route is followed to the apical surface.

CL3 is critical not only for trafficking of MRP1 but also the binding of substrates, such as LTC_4 and azidophenacyl-GSH (Gao et al., 1998; Qian et al., 2001a; Konno et al., 2003). Consequently, we determined how substitution of this region by fragments from MRP2 affected the function of the hybrid protein by examining transport of two well characterized organic anion substrates of MRP1 and MRP2 (LTC_4 and $E_2$17βG) and a third substrate ($E_1$3SO_4) which is transported only by MRP1. $MRP2_{1\text{-}319}/MRP1_{323\text{-}1531}$ displayed a V_{max} for LTC_4 transport very similar to that of MRP1, while the K_m of the hybrid was similar to that of MRP2 (i.e. ~10 fold higher than that of MRP1). Thus the relatively low sequence conservation of CL3 between MRP1 and MRP2 may contribute to the substantial difference in affinity that the two proteins display for this common substrate. Photolabeling with ^{35}S-labeled azidophenacyl GSH was also markedly diminished, consistent with studies indicating that MRP1 CL3 is important for binding this GSH derivative, as well as LTC_4 (Qian et al., 2001b, Qian et al., 2002).

We were unable to detect transport of either $E_2$17βG or $E_1$3SO_4 by $MRP2_{1\text{-}319}/MRP1_{323\text{-}1531}$ (Fig. 7C and Fig. 8A). Furthermore, exchange of only the COOH-proximal region of CL3 (aa 286-319) for the comparable region of MRP2 profoundly decreased transport of both conjugated steroids (75-90%) (Fig. 7C and Fig. 8A), but had little effect on LTC_4 transport (Fig. 7D and E) or binding of ^{35}S-labeled azidophenacyl GSH (Fig. 8B). Consequently, this region of MRP1 CL3 appears to be critical for binding of the two steroid conjugates but not for interaction with azidophenacyl GSH or the GSH conjugate LTC_4. Both MRP1 and MRP2 display reciprocal

competition between LTC_4 and $E_2$17βG, suggesting common or mutually exclusive binding sites for these substrates. Our present findings suggest that CL3 is important for interaction with both substrates, but that the regions involved are not identical.

Attempts to identify additional regions in MSD0 or CL3 that contributed to apical targeting of $MRP2_{1-319}/MRP1_{323-1531}$ were unsuccessful (Fig. 5). MRP1 hybrids containing MSD0 and the COOH-terminal region of CL3 from MRP2, or just MRP2 CL3 localized to both basolateral and apical membranes, as observed with a construct containing only $MRP2_{286-319}$. These and previous results using MRP1 hybrids in which MSD0 and only parts of CL3 had been exchanged, strongly suggest that the integrity of the entire region encompassing MSD0 and CL3 of MRP2 is required for efficient apical targeting. The fact that neither $MRP2_{1-319}$ nor $MRP1_{323-1531}$ (data not shown) traffic to the plasma membrane when expressed independently also suggests that interactions between the two heterologous fragments are required for the processing of the hybrid protein through the ER and for trafficking to the apical membrane.

One striking feature of the COOH-proximal region of MRP2 CL3 is the presence of a polybasic 10 amino acid motif containing 7 lysine residues (5 of which are consecutive), that is not present in any other mammalian MRPs (Fig. 1). While various point mutations of a single lysine (Lys296) in this motif did not affect the apical distribution of $MRP2_{1-319}/MRP1_{323-1531}$, exchange of the entire motif for the corresponding MRP1 sequence resulted in accumulation of the protein in a subapical intracellular compartment (Fig. 6). As observed when the more extended region of MRP2 from aa 290-319 was exchanged for the corespnding sequence from MRP1, none of the mutant protein was detected in the basolateral membrane.

Polybasic motifs have been implicated in membrane targeting of a wide variety of proteins, in part by virtue of their ability to form electrostatic interactions with phospholipids,

notably phosphatidyl inositols (Heo et al., 2006). Such regions have been implicated in the membrane association of the small GTPases Rit and Rin (Fivaz and Meyer, 2003), oncoproteins such as K-ras (Yeung et al., 2008), integral membrane proteins such as CD43 and ICAM-2 (Yonemura et al., 1998) and Myristoylated alanine-rich C kinase substrate (MARCKS) and MARCKS-related protein (Sundaram et al., 2004). Consistent with the possibility of such a role for the motif in MRP2, it is located in a predicted cytoplasmic, juxtamembrane region immediately NH_2-proximal to TM6.

In some cases, regulation of the interaction of polybasic regions with the membrane involves Ser/Thr phosphorylation by PKC, which is in turn is activated by PI hydrolysis (Sundaram et al., 2004; Yeung et al., 2008). MRP2 has been shown to be acutely regulated by PKC, activation of which results in rapid loss of the apical localization of MRP2 in liver and kidney (Kubitz et al., 2001). Analysis of CL3 of MRP2 orthologs from higher eukaryotes indicates that it contains a high probability (> 0.8), potential PKC site located in the lysine rich motif (KKKKK**S**G**T**KK) that is conserved in all vertebrates analyzed, including: rhesus monkey (KKKKKKSG**T**KK), dog (KKKKKKSG**TT**), mouse (**S**KKKKKKSEA**T**), rat (KKKSEK**T**TK) and zebra fish (**S**KKKKKKKQK). Polybasic regions are also found associated with binding sites for PDZ proteins. Although these sites are often located in the COOH-terminal region of the protein, this is not always the case (Hung and Sheng, 2002). The sequence immediately preceding the polybasic motif in the human protein contains two matches for Class III PDZ binding motifs (**QDAL**V**LEDV**EKKKKKSGTKK) the NH2-proximal of which is conserved in all available sequences of MRP2 from mammals and zebra fish. Given that it is possible to eliminate the PDZ binding motif in the COOH-tail of MRP2 without affecting apical targeting of

the protein, this region of CL3 may be an alternative candidate for mediating interaction with ERM proteins and PKC regulated membrane association.

Acknowledgments

We thank Monika Vasa and Ruth Burtch-Wright for assistance with tissue culture and cloning procedures, and Matt Gordon and Jeff Mewburn for assistance with microscopy and imaging.

References

Babenko AP and Bryan J (2003) SUR domains that associate with and gate K_{ATP} pores define a novel gatekeeper. *J Biol Chem* 278:41577-41580.

Bakos E, Evers R, Calenda G, Tusnády GE, Szakács G, Váradi A, Sarkadi B.(2000) Characterization of the amino-terminal regions in the human multidrug resistance protein (MRP1). J Cell Sci. 2000 Dec;113 Pt 24:4451-61.

Bakos E, Evers R, Szakacs G, Tusnady GE, Welker E, Szabo K, de Haas M, van Deemter L, Borst P, Varadi A and Sarkadi P (1998) Functional multidrug resistance protein (MRP1) lacking the NH2-terminal transmembrane domain. *J Biol Chem* 273:32167-32175.

Ciaccio PJ, Shen H, Kruh GD and Tew KD (1996) Effects of chronic ethacrynic acid exposure on glutathione conjugation and MRP expression in human colon tumor cells. *Biochem Biophys Res Commun* 222: 111-115.

Cole SPC, Bhardwaj G, Gerlach JH, Mackie JE, Grant CE, Almquist KC, Stewart AJ, Kurz EU, Duncan AM and Deeley RG (1992) Overexpression of a transporter gene in a multidrug-resistant human lung cancer cell line. *Science* 258:1650-1654.

CuiY, Konig J, Buchholz JK, Spring H, Leier I and Keppler D (1999) Drug resistance and ATP-dependent conjugate transport mediated by the apical multidrug resistance protein, MRP2, permanently expressed in human and canine cells. *Mol Pharmacol* 55: 929-937.

Deeley RG, Westlake C and Cole SPC (2006) Transmembrane transport of endo- and xenobiotics by mammalian ATP-binding cassette multidrug resistance proteins. *Physiol Rev* 86:849-899.

Fernandez SB, Hollo Z, Kern A, Bakos E, Fischer PA, Borst P and Evers R (2002) Role of the NH2-terminal transmembrane region of the multidrug resistance protein MRP2 in routing to the apical membrane in MDCKII cells. *J Biol Chem* 277:31048-31055.

Fivaz M and Meyer T (2003) Specific localization and timing in neuronal signal transduction mediated by protein-lipid interactions. *Neuron* 40:319-330.

Gao M, Loe DW, Grant CE, Cole SPC and Deeley RG (1996) Reconstitution of ATP-dependent leukotriene C_4 transport by co-expression of both half-molecules of human multidrug resistance protein in insect Sf21 cells. *J Biol Chem* 271:27782-27787.

Gao M, Yamazaki M, Loe DW, Westlake CJ, Grant CE, Cole SPC and Deeley RG (1998) Multidrug resistance protein: identification of regions required for active transport of leukotriene C_4. *J Biol Chem* 273:10733-10740.

Hegedus T, Sessler T, Scott R, Thelin W, Bakos E, Varadi A, Szabo K, Homolya L, Milgram SL and Sarkadi B (2003) COOH-terminal phosphorylation of MRP2 modulates its interaction with PDZ proteins. *Biochem Biophys Res Commun* 302:454-461.

Heo WD, Inoue T, Park WS, Kim ML, Park BO, Wandless TJ, Meyer T (2006) PI(3,4,5)P3 and PI(4,5)P2 lipids target proteins with polybasic clusters to the plasma membrane. *Science* 314:1458-1461.

Hipfner DR, Almquist KC, Leslie EM, Gerlach JH, Grant CE, Deeley RG and Cole SPC (1997) Membrane topology of the multidrug resistance protein (MRP): a study of glycosylation-site mutants reveals an extracytosolic NH_2 terminus. *J Biol.Chem* 272:23623-23630.

Hipfner DR, Gao M, Scheffer G, Scheper RJ, Deeley RG and Cole SPC (1998) Epitope mapping of monoclonal antibodies specific for the 190-kDa multidrug resistance protein (MRP). *Br J Cancer* 78:1134-1140.

Hung Y and Sheng M (2002) PDZ domains: Structural modules for protein complex assembly. *J Biol Chem* 277:5699-5702.

Ito K, Oleschuk CJ, Westlake C, Vasa MZ, Deeley RG and Cole SPC (2001) Mutation of Trp^{1254} in the multispecific organic anion transporter, multidrug resistance protein 2 (MRP2) (ABCC2), alters substrate specificity and results in loss of methotrexate transport activity. *J Biol Chem* 276:38108-38114.

Ito K, Weigl KE, Deeley RG and Cole SPC (2003) Mutation of proline residues in the NH(2)-terminal region of the multidrug resistance protein, MRP1 (ABCC1): effects on protein expression, membrane localization, and transport function. *Biochim Biophys Acta* 1615:103-114.

Keppler D, Leier I and Jedlitschky G (1997) Transport of glutathione conjugates and glucuronides by the multidrug resistance proteins MRP1 and MRP2. *Biol Chem* 378:787-791.

Kikuchi S, Hata M, Fukumoto K, Yamane Y, Matsui T, Tamura A, Yonemura S, Yamagishi H, Keppler D, Tsukita S and Tsukita S (2002) Radixin deficiency causes conjugated hyperbilirubinemia with loss of Mrp2 from bile canalicular membranes. *Nat Genet* 31:320-325.

Konno T, Ebihara T, Hisaeda K, Uchiumi T, Nakamura T, Shirakusa T, Kuwano M and Wada M (2003) Identification of domains participating in the substrate specificity and subcellular localization of the multidrug resistance proteins MRP1 and MRP2. *J Biol Chem* 278:22908-22917.

Kubitz R, Huth C, Schmitt M, Horbach A, Kullak-Ublick G and Häussinger D (2001) Protein kinase C-dependent distribution of the multidrug resistance protein 2 from the canalicular to the basolateral membrane in human HepG2 cells. *Hepatology* 34:340-350.

Leonard GD, Fojo T and Bates SE (2003) The role of ABC transporters in clinical practice. *Oncologist* 8:411-424.

Leslie EM, Bowers RJ, Deeley RG and Cole SPC (2003) Structural requirements for functional interaction of glutathione tripeptide analogs with the human multidrug resistance protein 1 (MRP1). *J Pharmacol Exp Ther* 304:643-653.

Leslie EM, Deeley RG and Cole SPC (2001) Toxicological relevance of the multidrug resistance protein 1, MRP1 (ABCC1) and related transporters. *Toxicology* 167:3-23.

Loe DW, Almquist KC, Cole SPC and Deeley RG (1996) ATP-dependent 17β-estradiol 17-(β-D-glucuronide) transport by multidrug resistance protein (MRP): inhibition by cholestatic steroids. *J Biol Chem* 271:9683-9689.

Mason DL and Michaelis S (2002) Requirement of the NH2-terminal extension for vacuolar trafficking and transport activity of yeast Ycf1p, an ATP-binding cassette transporter. *Mol Biol Cell* 13:4443-4455.

Nies AT, Konig J, Cui Y, Brom M, Spring H and Keppler D (2002) Structural requirements for the apical sorting of human multidrug resistance protein 2 (ABCC2). *Eur J Biochem* 269:1866-1876.

Paulusma CC, Kool M, Bosma PJ, Scheffer GL, Borg F, Scheper RJ, Tytgat GN, Borst P, Baas F and Oude Elferink RP **(**1997) A mutation in the human canalicular multispecific organic anion transporter gene causes the Dubin-Johnson syndrome. *Hepatology* 25:1539–1542.

Paulusma CC, van Geer MA, Evers R, Heijn M, Ottenhoff R, Borst P and Oude Elferink RP (1999) Canalicular multispecific organic anion transporter/multidrug resistance protein 2 mediates low-affinity transport of reduced glutathione. *Biochem J* 338 (Pt 2):393-401.

Qian YM, Grant CE, Westlake CJ, Zhang DW, Lander PA, Shepard RL, Dantzig AH, Cole SPC and Deeley RG (2002) Photolabeling of human and murine multidrug resistance protein 1 with the high affinity inhibitor [^{125}I]LY475776 and azidophenacyl-[^{35}S]glutathione. *J Biol Chem* 277:35225-35231.

Qian YM, Qiu W, Gao M, Westlake CJ, Cole SPC and Deeley RG (2001a) Characterization of binding of leukotriene C_4 by human multidrug resistance protein 1: evidence of differential interactions with NH_2- and COOH-proximal halves of the protein. *J Biol Chem* 276:38636-38644.

Qian YM, Song WC, Cui H, Cole SPC and Deeley RG (2001b) Glutathione stimulates sulfated estrogen transport by multidrug resistance protein 1. *J Biol Chem* 276:6404-6411.

Roush DL, Gottardi CJ, Naim HY, Roth MG and Caplan MJ (1998) Tyrosine-based membrane protein sorting signals are differentially interpreted by polarized Madin-Darby canine kidney and LLC-PK_1 epithelial cells. *J Biol Chem* 273:26862-26869

Sundaram M, Cook HW and Byers DM (2004) The MARCKS family of phospholipid binding proteins: regulation of phospholipase D and other cellular components. *Biochem Cell Biol* 82:191-200.

Tusnady GE, Bakos E, Varadi A and Sarkadi B (1997) Membrane topology distinguishes a subfamily of the ATP-binding cassette (ABC) transporters. *FEBS Lett* 402:1-3.

Van Aubel RA, Hartog A, Bindels RJ, Van Os CH and Russel FG (2000) Expression and immunolocalization of multidrug resistance protein 2 in rabbit small intestine. *Eur J Pharmacol* 400: 195-198.

Westlake CJ, Cole SPC and Deeley RG (2005) Role of the NH_2-terminal membrane spanning domain of multidrug resistance protein 1/ABCC1 in protein processing and trafficking. *Mol Biol Cell* 16:2483-2492.

Westlake CJ, Payen L, Gao M, Cole SPC and Deeley RG (2004) Identification and characterization of functionally important elements in the multidrug resistance protein 1 COOH-terminal region. *J Biol Chem* 279: 53571-53583.

Westlake CJ, Qian YM, Gao M, Vasa M, Cole SPC and Deeley RG (2003) Identification of the structural and functional boundaries of the multidrug resistance protein 1 cytoplasmic loop 3. *Biochemistry* 42:14099-14113.

Yeung T, Gilbert GE, Shi J, Silvius J, Kapus A and Grinstein S (2008) Membrane phosphatidylserine regulates surface charge and protein localization. *Science* 319:210-213.

Yonemura S, Hirao M, Doi Y, Takahashi N, Kondo T, Tsukita S and Tsukita S (1998) Ezrin/radixin/moesin (ERM) proteins bind to a positively charged amino acid cluster in the juxta-membrane cytoplasmic domain of CD44, CD43, and ICAM-2. *J Cell Biol* 140:885-895.

Footnotes:

This work was supported by a grant from the Canadian Institutes of Health Research (MOP-62824).

[1]*Current address: Department of Chemistry & Chemical Engineering, Royal Military College of Canada, P.O. Box 17000, Stn. Forces, Kingston, ON, K7K 7B4 (P.E.B.);* [2]*Genentech Inc., 1 DNA Way South, San Francisco, CA 94080 (C.J.W.)*

Legends for Figures

Fig. 1. Sequence alignment of CL3 and the cytoplasmic NH2-terminal regions of various ABCC proteins. The alignment was performed with Clustal W v1.83 using a gap open penalty of 10 and a gap extension penalty of 0.05. The entire sequence of each protein was used to generate the initial alignment. Highly conserved aa are indicated with vertical rectangles and the positions of two previously identified, broadly conserved α-helices are also shown (Westlake et al., 2003). A polybasic motif unique to MRP2 is shown in bold within a horizontal rectangle. The position of Lys^{296} which was subjected to site-directed mutagenesis (see text 'Results' and Fig. 6) is indicated by an asterisk).

Fig. 2. Structures of MRP1/MRP2 hybrid proteins. Cartoons of predicted topologies of various MRP1/MRP2 hybrids referred to in the text are shown with regions from MRP2 and MRP1 indicated in black and gray, respectively. The amino acid positions of each protein that form the sites used to connect various fragments of MRP1 and MRP2 are also indicated.

Fig. 3. Membrane localization of wild-type MRP1 and MRP2 expressed in polarized MDCK-1 and LLC PK1 cell lines. MRP1 and MRP2 were expressed in stable MDCK-1 and transient LLC-PK1 transfectants and detected with mAb MRPr1 (A) or mAb $M2_{I-4}$ (B) (green), respectively. Cells were also stained with an antibody to the endoplasmic reticulum marker, calnexin (red). Nuclei were counterstained with Hoechst 33342 (blue). Arrows indicate the location of xz-section shown below each panel. Scale bar represents 10 μm. Magnification was 126 fold.

Fig. 4. Expression and trafficking of MRP1/MRP2 hybrids in MDCK-1 and LLC-PK1 cells: Confocal microscopy analysis of fixed cells was performed on stable MDCK-1 transfectants and transient LLC-PK1 transfectants after immunostaining with MRP2-specific mAb $M2_{I-4}$ (A and B) or MRP1-specific mAb MRPr1 (C) (green). Cells were also stained with an antibody to the endoplasmic reticulum marker, calnexin (red). Nuclei were counterstained with Hoechst 33342 (blue). Panel A) construct $MRP2_{1-289}/MRP1_{291-1531}$ (Fig. 2B); Panel B) construct $MRP2_{1-319}/MRP1_{323-1531}$ (Fig.2A) and Panel C) construct $MRP1_{1-290}/MRP2_{286-319}/MRP1_{323-1531}$ (Fig. 2C). Arrows indicate the location of xz-sections below each panel. Scale bars represent 10 μm. Magnification was 126 fold.

Fig. 5. Expression and trafficking of additional MRP1/MRP2 hybrids and $MRP2_{1-319}$ in MDCK-1 and LLC-PK1 cells. Confocal microscopy and immunostaining of MDCK-1 and LLC-PK1 transient transfectants was performed as in Fig. 4. Hybrids were detected with MRP2-specific mAb $M2_{I-4}$ (panels A, C and D) or the MRP1-specific mAb MRPr1 (panel B). Panel A) $MRP2_{1-289}/MRP1_{291-322}/MRP2_{320-1546}$ (Fig. 2D); Panel B) $MRP2_{1-187}/MRP1_{204-290}/MRP2_{286-319}/MRP1_{323-1531}$ (Fig. 2F); Panel C) $MRP1_{1-203}/MRP2_{189-319}/MRP1_{323-1531}$ (Fig. 2E) and Panel D) $MRP2_{1-319}$ (Fig. 2G).

Fig. 6. Impact of mutations in the basic motif in MRP2 CL3 on the apical localization of $MRP2_{1-319}/MRP1_{323-1531}$ in transiently transfected MDCK-1 cells. The Lys residue at position 296 in the middle of a stretch of 5 Lys residues in the polybasic motif identified in MRP2 (Fig. 1) was mutated to Arg (top left), Gln (top right) or Glu (bottom left) in the $MRP2_{1-319}/MRP1_{323-}$

$_{1531}$ hybrid. The whole motif (aa 294-303) was also exchanged in this hybrid for the corresponding MRP1 sequence (aa 299-308) (bottom right). All mutants were transiently expressed in MDCK-1 cells. Cells were fixed 48 hr after transfection and immunostained with MRP2-specific mAb $M2_{I-4}$ (green). Cells were also stained for calnexin (red) and nuclei were counterstained (blue) as in Fig. 4. White arrows indicate location of xz-sections. Confocal microscopy was as described in Fig.4.

Fig. 7. Activity of MRP1/MRP2 hybrid proteins expressed in Sf21 insect membrane vesicles. (A) Immunoblot of wild-type MRP1 and MRP1/MRP2 hybrid proteins (only MRP2 regions are indicated) following SDS-PAGE of Sf21 membrane vesicles (1.0 μg total protein) probed with mAb MRPm6 as described in *Material and Methods*. (B) Slot blot of wild-type MRP1, hybrids and β-glucuronidase (β-gus) (negative control) expressed in Sf21 membrane vesicles (1.5, 1.0 and 0.5 μg total protein), probed with mAb MRPm6. (C) ATP-dependent uptake of [^{3}H]$E_2$17βG (400 nM) after incubation at 37^{o}C for 1 min (open bars) or 5 min (closed bars) by Sf21 membranes vesicles expressing MRP1, MRP2 or hybrids (6 μg total protein). (D) Time course of ATP-dependent uptake of [^{3}H]LTC_4 by Sf21 membrane vesicles expressing wild-type MRP1 (■) or hybrids $MRP2_{286-319}$ (▼) or $MRP2_{1-319}$ (▲) at 23^{o}C. (E) LTC_4 transport kinetics were determined by incubating Sf21 vesicles at 23^{o}C for 30 sec in the presence of different concentrations (25-600 nM) of [^{3}H]LTC_4. (E) *inset*, Hanes-Woolf transformation of the data from which kinetic parameters were determined. In all cases, ATP-dependent uptake of substrates into inside-out vesicles was normalized to relative protein expression levels in panel B. Panels D and E are pooled results of 2 experiments with the same membrane preparations. Some error bars are contained within the limits of the symbol.

Fig. 8. Azidophenacyl-[^{35}S]GSH photolabeling and S-methyl GSH stimulated E_13SO_4 transport by wild-type MRP1 and MRP1/MRP2 hybrids. (A) E_13SO_4 uptake was measured using Sf21 vesicles (4 μg total protein) expressing wild-type MRP1 or MRP1/MRP2 hybrids in the presence of 2 mM S-methyl GSH at 37^{o}C for 3 min. (B) Autoradiograph of Sf21 membrane vesicles containing wild-type MRP1 (75 μg) or equivalent amounts of vesicles containing MRP1/MRP2 hybrids and β-gus after photolabeling with azidophenacyl-[^{35}S]GSH as described in *Material and Methods.* Membrane proteins were resolved by SDS-PAGE using a 6% gel. (C) Immunoblot of equivalent aliquots of membrane preparations used for photolabeling studies (panel B) resolved SDS-PAGE using a 7.5% gel.

Table 1: Hybrid cloning strategies for cDNAs used in membrane trafficking studies. Listed are the restriction endonucleases, MRP1 and MRP2 PCR templates and primers used for generating the MRP1/MRP2 chimeric cDNAs. Where indicated cDNAs were prepared by recombinant PCR.

Name	Amplified cDNA fragment (corresponding amino acids)	Template***	Primers* **BOLD** – indicates primers used in recombinant PCR step	Insertion – vector backbone
MRP2(1-319)/ MRP1(323-1531)	MRP2 (1-319)	MRP2	**F: GCCGCCATGCTGGAGAAGTTCTGCAAC** R: GTAGAAAGTTTTGAACAGAGC	HindIII/PshAI – MRP1
	MRP1 (323-1531)	MRP1	F: GTTCAAAACTTTCTAGCCCTACTTCCTCATGAGCTTCTTC **R: GTAGGCAGACTTCTTCAGC**	
MRP2(1-289)/ MRP1(291-1531)	MRP2(1-289)	MRP2	**F: CACAAGCTTGCCGCCATGCTGGAGAAGTTCTGCAAC** R: CCAGGACAAGGGCATC	BsrGI/PshAI – MRP2(1-319)/ MRP1(323-1531)
	MRP1(291-1531)	MRP1	F: GATGCCCTTGTCCTGGTGGATGCGAATGAGGAGG **R: GTAGGCAGACTTCTTCAGC**	
MRP1(1-290)/ MRP2(286-319)/ MRP1(232-1531)	MRP1(1-290)	MRP1	**F: GCTCTCTGGCTAACTAGAGAACC**** R: CCTTGGAACTCTCTTTCGG	NheI/PshAI – MRP2(1-319)/ MRP1(323-1531)
	MRP2(286-319)/MRP1(323-1531)	MRP2(1-319)/ MRP1(323-1531)	F: CGAAAGAGAGTTCCAAGGCCCTTGTCCTGGAAGATGTT **R: GTAGGCAGACTTCTTCAGC**	
MRP2(1-289)/ MRP1(291-322)/ MRP2(320-1545)	MRP2(1-289)/MRP1(291-322)	MRP2(1-289)/ MRP1(291-1531)	**F: GCCGCCATGCTGGAGAAGTTCTGCAAC** R: GCACCATGGGCCCAAAGGTCTTGTA	BsrGI/ HpaI – MRP2
	MRP2(320-1545)	MRP2	F: CCTTTGGGCCCATGGTGCTCCTGAAATCATTCC **R: CTACAATCTCATCCACTTGAGG**	
MRP2(1-187)/ MRP1(204-290)/ MRP2(286-319)/ MRP1(323-1531)	MRP2(1-187)/MRP1(204-290)	MRP2(1-187)/ MRP1(204-1531) (Westlake et.al. 2005)	**F: GCTCTCTGGCTAACTAGAGAACC**** R: CCTTGGAACTCTCTTTCGG	NheI/PshAI - MRP2(1-319)/ MRP1(323-1531)
	MRP2(286-319)/MRP1(323-1531)	MRP1(1-290)/ MRP2(286-319)/ MRP1(232-1531)	F: CGAAAGAGAGTTCCAAGGCCCTTGTCCTGGAAGATGTT **R: GTAGGCAGACTTCTTCAGC**	

* Underlined portion of primers corresponds to respective overlapping regions in DNA fragments used in the recombinant PCR step to generate hybrid junctions.
** Forward primer epitope is in pcDNA3.1(-) vector; *** All cDNA templates used for PCR were in pcDNA3.1(-)

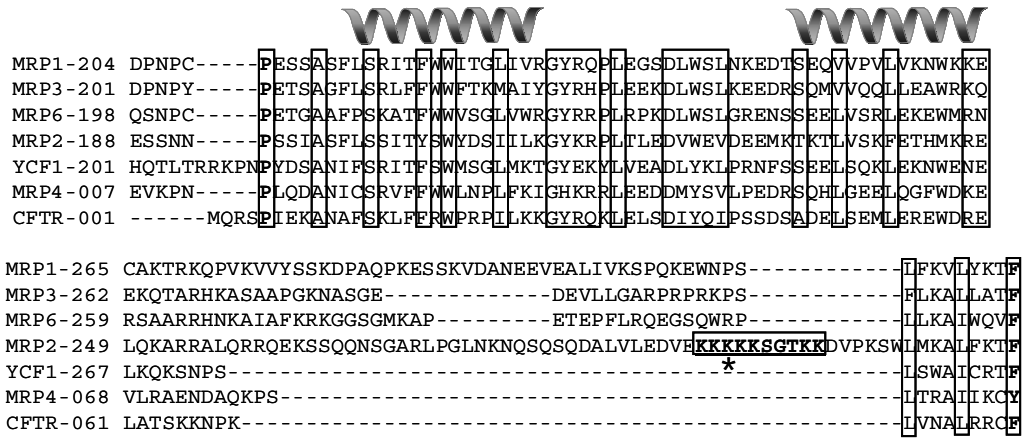
MRP1-204 DPNPC-----PESSASFLSRITFWWITGLIVRGYRQPLEGSDLWSLNKEDTSEQVVPVLVKNWKKE
MRP3-201 DPNPY-----PETSAGFLSRLFFWWFTKMAIYGYRHPLEEKDLWSLKEEDRSQMVVQQLLEAWRKQ
MRP6-198 QSNPC-----PETGAAFPSKATFWWVSGLVWRGYRRPLRPKDLWSLGRENSSEELVSRLEKEWMRN
MRP2-188 ESSNN-----PSSIASFLSSITYSWYDSIILKGYKRPLTLEDVWEVDEEMKTKTLVSKFETHMKRE
YCF1-201 HQTLTRRKPNPYDSANIFSRITFSWMSGLMKTGYEKYLVEADLYKLPRNFSSEELSQKLEKNWENE
MRP4-007 EVKPN-----PLQDANICSRVFFWWLNPLFKIGHKRRLEEDDMYSVLPEDRSQHLGEELQGFWDKE
CFTR-001 ------MQRSPIEKANAFSKLFFRWPRPILKKGYRQKLELSDIYQIPSSDSADELSEMLEREWDRE
MRP1-265 CAKTRKQPVKVVYSSKDPAQPKESSKVDANEEVEALIVKSPQKEWNPS----------TFKVLYKTF
MRP3-262 EKQTARHKASAAPGKNASGE----------DEVLLGARPRPRKPS----------FLKALLATF
MRP6-259 RSAARRHNKAIAFKRKGGSGMKAP---------ETEPFLRQEGSQWRP----------LLKAIWQVF
MRP2-249 LQKARRALQRRQEKSSQQNSGARLPGLNKNQSQSQDALVLEDVEKKKKKSGTKKDVPKSWLMKALFKTF
YCF1-267 LKQKSNPS----------*----------LSWAICRTF
MRP4-068 VLRAENDAQKPS----------ITRAIIKCY
CFTR-061 LATSKKNPK----------LVNALRRCF

Figure 1

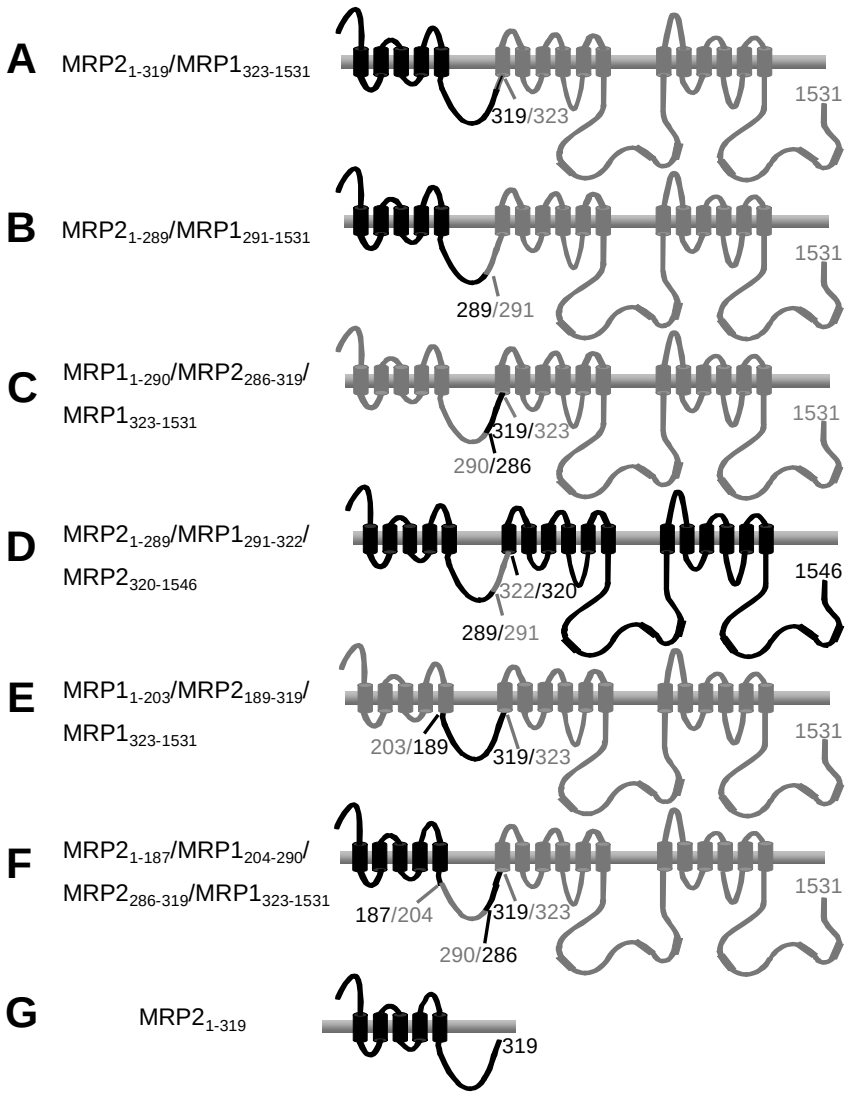
A
MRP2$_{1-319}$/MRP1$_{323-1531}$
319/323
1531
B
MRP2$_{1-289}$/MRP1$_{291-1531}$
289/291
1531
C
MRP1$_{1-290}$/MRP2$_{286-319}$/
MRP1$_{323-1531}$
319/323
290/286
1531
D
MRP2$_{1-289}$/MRP1$_{291-322}$/
MRP2$_{320-1546}$
322/320
289/291
1546
E
MRP1$_{1-203}$/MRP2$_{189-319}$/
MRP1$_{323-1531}$
203/189
319/323
1531
F
MRP2$_{1-187}$/MRP1$_{204-290}$/
MRP2$_{286-319}$/MRP1$_{323-1531}$
187/204
319/323
290/286
1531
G
MRP2$_{1-319}$
319

Figure 2

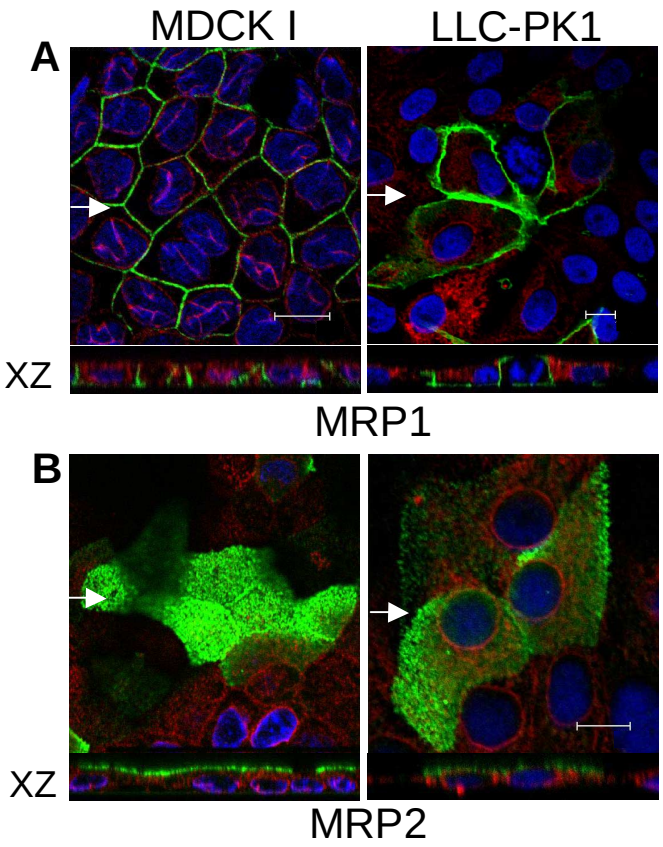

Figure 3

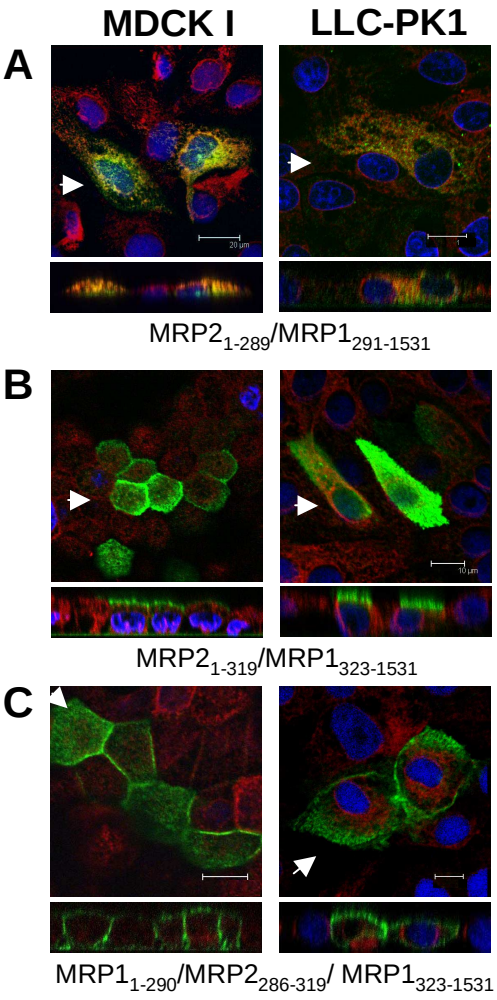
MDCK I
LLC-PK1
A
MRP2$_{1-289}$/MRP1$_{291-1531}$
B
MRP2$_{1-319}$/MRP1$_{323-1531}$
C
MRP1$_{1-290}$/MRP2$_{286-319}$/ MRP1$_{323-1531}$

Figure 4

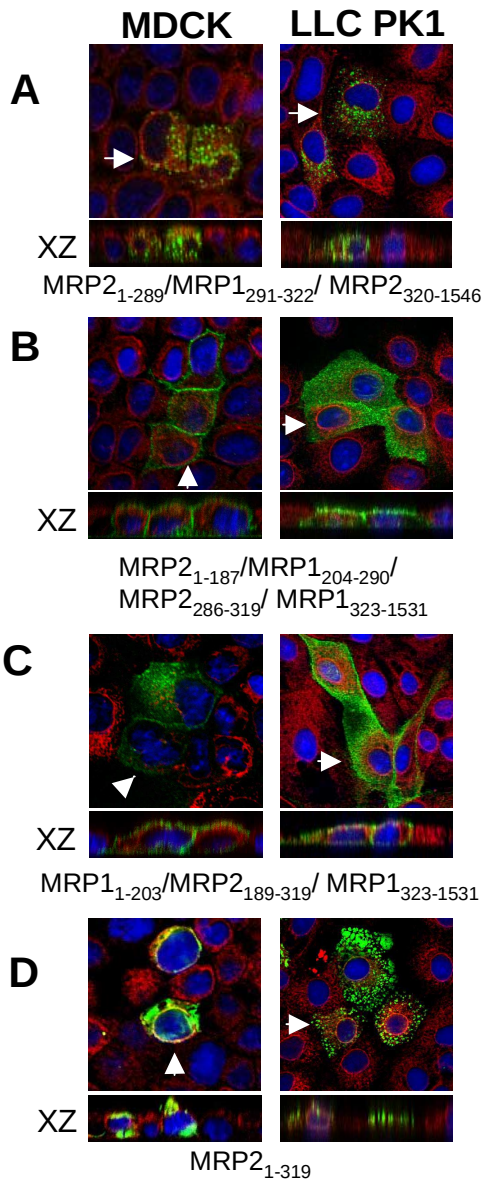
MDCK
LLC PK1
A
XZ
MRP2$_{1-289}$/MRP1$_{291-322}$/ MRP2$_{320-1546}$
B
XZ
MRP2$_{1-187}$/MRP1$_{204-290}$/
MRP2$_{286-319}$/ MRP1$_{323-1531}$
C
XZ
MRP1$_{1-203}$/MRP2$_{189-319}$/ MRP1$_{323-1531}$
D
XZ
MRP2$_{1-319}$

Figure 5

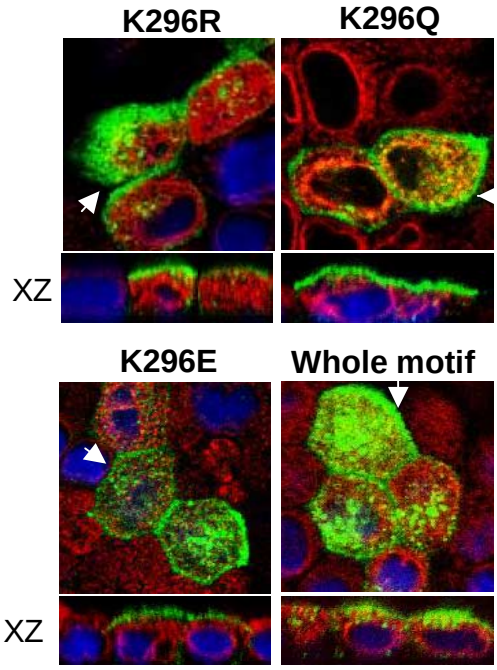

Figure 6

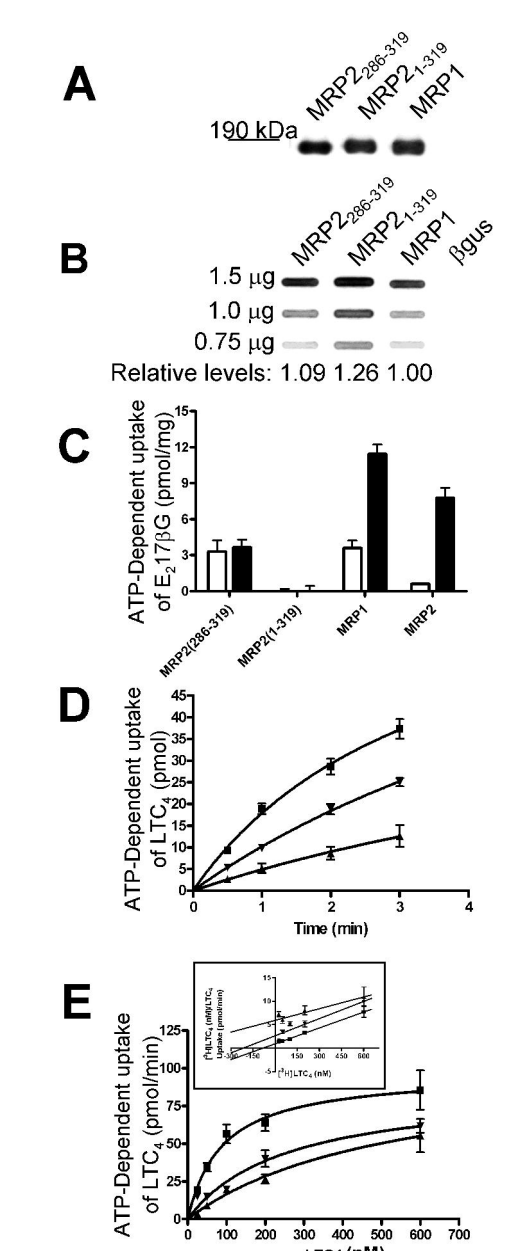
A
MRP2286-319
MRP21-319
MRP1
190 kDa
B
MRP2286-319
MRP21-319
MRP1
βgus
1.5 μg
1.0 μg
0.75 μg
Relative levels: 1.09 1.26 1.00
C
ATP-Dependent uptake of E2 17βG (pmol/mg)
MRP2(286-319)
MRP2(1-319)
MRP1
MRP2
D
ATP-Dependent uptake of LTC4 (pmol)
Time (min)
E
ATP-Dependent uptake of LTC4 (pmol/min)
LTC4 (nM)

Figure 7

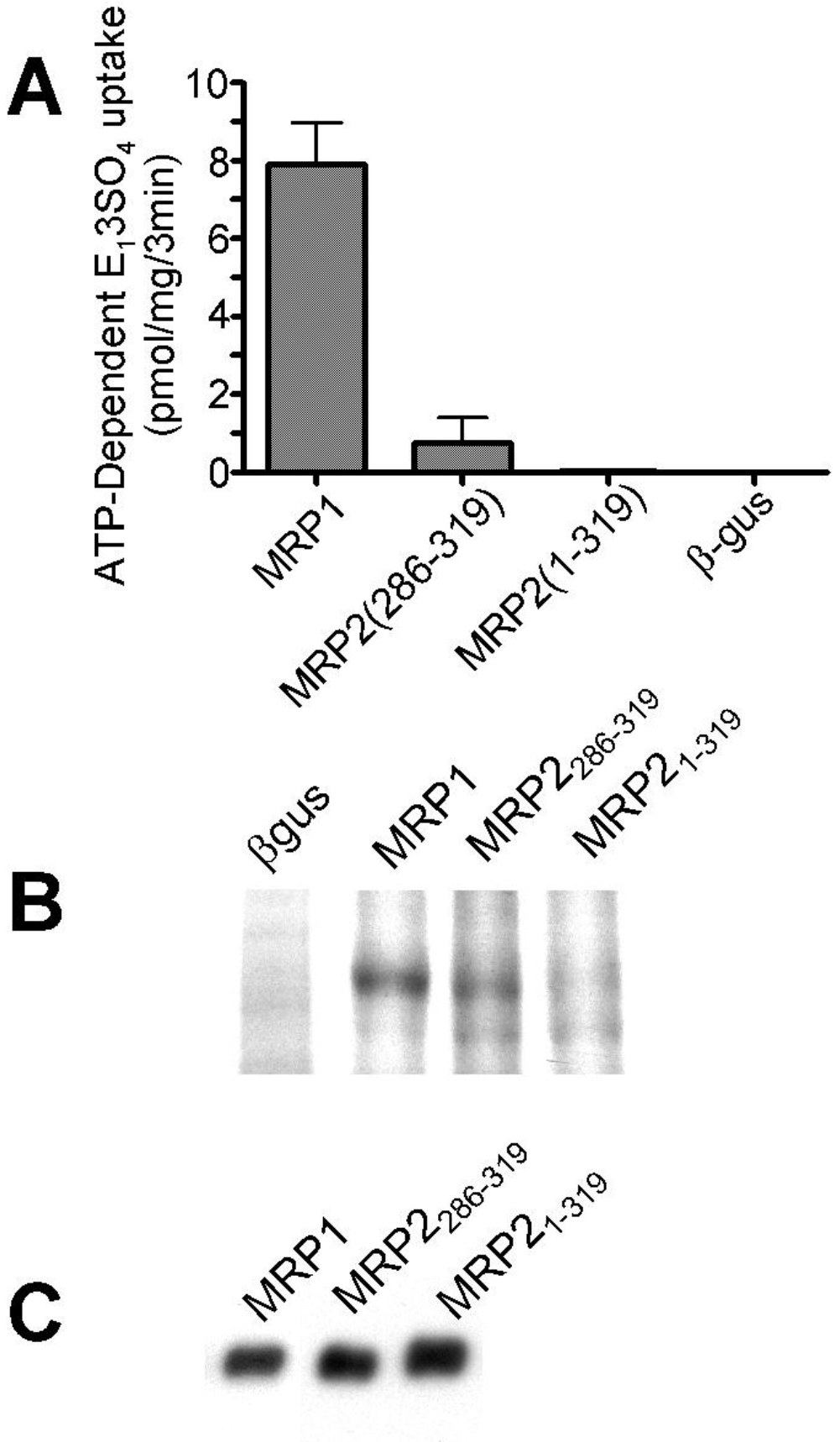
A
ATP-Dependent E1 3SO4 uptake
(pmol/mg/3min)
10
8
6
4
2
0
MRP1
MRP2(286-319)
MRP2(1-319)
β-gus
B
βgus
MRP1
MRP2286-319
MRP21-319
C
MRP1
MRP2286-319
MRP21-319

Figure 8